Low friction along the high slip patch of the 2011 Mw 9.0 Tohoku-Oki earthquake required from the wedge structure and extensional splay faults

Nadaya Cubas, Jean-Philippe Avouac, Yves M. Leroy, Adeline P Pons

Low friction along the high slip patch of the 2011 Mw 9.0 Tohoku-Oki earthquake required from the wedge structure and extensional splay faults

N. Cubas,[1] J. P. Avouac,[1] Y. M. Leroy,[2] and A. Pons[2]

Received 28 May 2013; revised 18 June 2013; accepted 18 June 2013.

[1] We analyze the mechanical properties needed to account for the large shallow slip during the 2011 Tohoku-Oki earthquake and the activation of landward normal faulting within the forearc. We show that the morphology and internal structure of the forearc follows closely the prediction of the critical Coulomb wedge in horizontal compression, implying a high internal pore pressure ratio ($\lambda = 0.7 + 0.14/ - 0.48$) and a low effective basal friction ($\mu_b^{\text{eff}} = 0.14 + 0.18/ - 0.04$). We then show that the activation of the normal fault requires a lower effective basal friction beneath the outer wedge than beneath the inner wedge ($\mu_{\text{outer}} \leq 0.015$), possibly due to transient dynamic weakening associated to the seismic rupture. Forearc normal faults could be considered as evidence for very efficient dynamic weakening along the megathrust and typify megathrust with high tsunamigenic potential.
Citation: Cubas, N., J. P. Avouac, Y. M. Leroy, and A. Pons (2013), Low friction along the high slip patch of the 2011 Mw 9.0 Tohoku-Oki earthquake required from the wedge structure and extensional splay faults, *Geophys. Res. Lett.*, *40*, doi:10.1002/grl.50682.

1. Introduction

[2] The 11 March 2011 Mw 9.0 Tohoku-Oki earthquake ruptured the plate interface between the Pacific Plate and NE Japan generating very large slip, probably exceeding 50 m at depth between 10 and 15 km, and a major tsunami [*Ozawa et al.*, 2011; *Wei et al.*, 2012; *Ide et al.*, 2011; *Simons et al.*, 2011, and Figure 1a]. Large shallow slip is attested from the displacement of ocean bottom gauges [*Ito et al.*, 2011] and comparison of bathymetric profiles measured in 1999 and late March 2011 [*Fujiwara et al.*, 2011]. While many magnitude 7.5 earthquakes had occurred along the deeper portion of the Megathrust, the large shallow slip came as a surprise since (1) the upper portion of the Megathrust is commonly thought to slip aseismically [e.g., *Oleskevich et al.*, 1999] and (2) interseismic strain accumulation models were not showing a locked patch near the trench [*Hashimoto et al.*, 2009; *Loveless and Meade*, 2011]. Another intriguing observation is that the earthquake activated a landward dipping normal fault [*Ito et al.*, 2011; *Tsuji et al.*, 2011, 2013], which lies slightly updip of the maximum slip area (Figure 1a). The landward normal fault marks the lower limit of an outer wedge formed by a stack of thrust sheets (Figure 1e). The fault, which extends parallel to the trench for several tens of kilometers, could have contributed to the tsunami [*Tsuji et al.*, 2011, 2013; *McKenzie and Jackson*, 2012], and its activation is consistent with the trench-perpendicular horizontal extension of the hanging wall revealed by aftershocks [*Ide et al.*, 2011; *Asano et al.*, 2011, and Figure 1c]. In this study, we analyze the mechanical properties of the wedge and Megathrust which are required to allow large shallow slip and activation of that normal fault. We show that the outer wedge morphology is consistent with a critical Coulomb wedge in horizontal compression [*Davis et al.*, 1983] and derive constraints on basal friction, internal friction, and pore pressure. We test next the possibility that the wedge would have reached the extensional critical limit as a result of coseismic stress change [*Kimura et al.*, 2012; *Conin et al.*, 2012]. We then evaluate the possibility that the localized normal faulting would be related to variation of frictional properties using the limit analysis approach [*Salençon*, 2002; *Maillot and Leroy*, 2006].

2. Frictional Properties Derived From the Critical Wedge Theory

[3] We focus on the epicentral area of the Tohoku-Oki earthquake (box in Figure 1a). We observe that the outer wedge morphology (Figure 1d) follows the prediction of the critical Coulomb wedge theory that the topographic slope is approximately a linear function of the dip angle of the Megathrust [e.g., *Suppe*, 2007] (Figure 2a). This theory allows relating the geometry of a wedge to the frictional properties of the bulk material and of the décollement [*Davis et al.*, 1983]. Depending on the topographic slope α and the Megathrust dip angle β, three domains are defined (Figure 2a):

[4] 1. A critical state. The Megathrust and the whole wedge are at the verge of failure, implying active faulting within the wedge, in horizontal compression for the lower branch of the envelope, and in horizontal extension for the upper branch.

[5] 2. A stable state within the critical envelope. In that state, the wedge can slide along the décollement without any permanent internal deformation.

[6] 3. Outside the critical envelope. The state of stress within the wedge would exceed the Coulomb yield criterion and is therefore forbidden in steady state in principle.

Additional supporting information may be found in the online version of this article.

[1]Tectonics Observatory, Division of Geological and Planetary Sciences, California Institute of Technology, Pasadena, California, USA.
[2]Laboratoire de Géologie, Ecole Normale Supérieure, Paris, France.

Corresponding author: N. Cubas, Tectonics Observatory, Division of Geological and Planetary Sciences, California Institute of Technology, 1200 E. California Blvd, Pasadena, CA 91125, USA. (cubas@caltech.edu)

0094-8276/13/10.1002/grl.50682

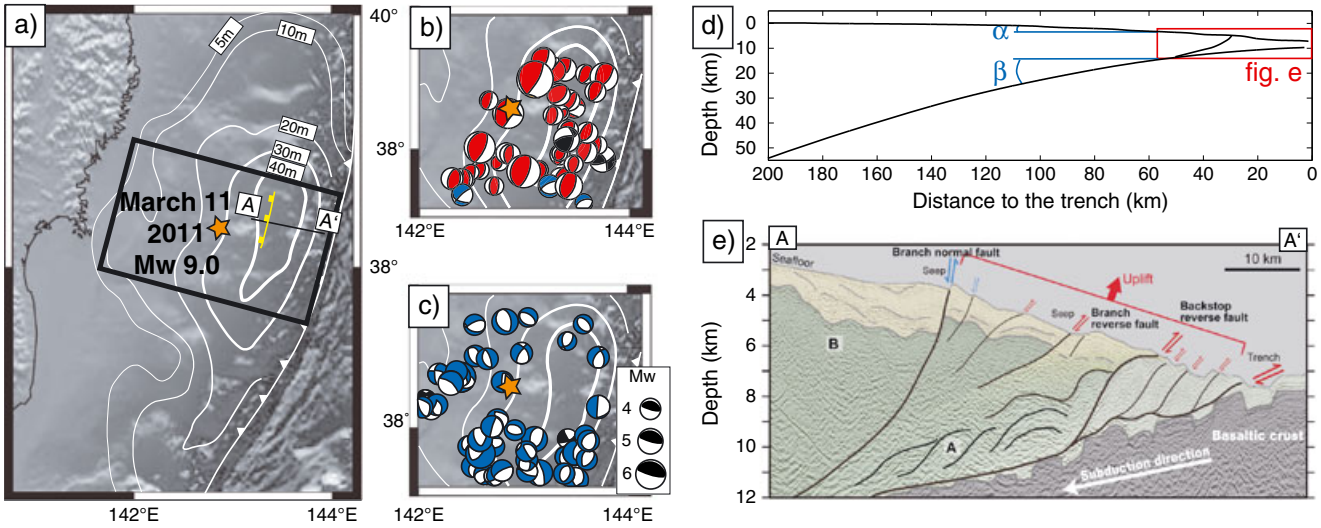

Figure 1. (a) Coseismic slip of the March 2011 Tohoku-Oki earthquake [*Wei et al.*, 2012] with location of the landward normal fault described by *Tsuji et al.* [2011]. The main shock epicenter is indicated by the star. Box shows area considered in the analysis of the wedge geometry in Figure 1d. (b) Spatial distribution of CMTs of earthquakes before the main shock (from January 2003 to 11 March 2011), and (c) noninterplate aftershocks in the hanging wall (from 11 to 24 March 2011) in the studied area from *Asano et al.* [2011]. Compression (red), extension (blue), strike-slip (black). (d) 150 km large swath profile with α the topographic slope, β the megathrust dip, and location of the landward normal fault. (e) Seismic reflection profile from *Tsuji et al.* [2011].

[7] We resort to this theory to identify the section of the forearc at criticality and place constraints on the mechanical properties of the forearc and Megathrust. We use the solution of *Dahlen* [1984] describing the critical taper angle formed by the topographic slope α and the Megathrust dip β as a function of the angle Ψ_B formed by the maximum principal stress σ_1 and the base of the wedge and the angle Ψ_0 formed by σ_1 and the top of a cohesionless wedge. For the lower compressive branch case, this relation reads as follows:

$$(\alpha + \beta)_c = \Psi_B - \Psi_0 \tag{1}$$

with

$$\Psi_B = \frac{1}{2}\arcsin\left(\frac{\sin\phi_b'}{\sin\phi_b}\right) - \frac{1}{2}\phi_b', \tag{2}$$

$$\Psi_0 = \frac{1}{2}\arcsin\left(\frac{\sin\alpha'}{\sin\phi}\right) - \frac{1}{2}\alpha'. \tag{3}$$

[8] The angles ϕ and ϕ_b are the internal and basal coefficients of friction defined as $\mu = \tan\phi$ and $\mu_b = \tan\phi_b$, and

$$\phi_b' = \arctan\left[\left(\frac{1-\lambda_b}{1-\lambda}\right)\tan\phi_b\right], \tag{4}$$

$$\alpha' = \arctan\left[\left(\frac{1-\rho_w/\rho}{1-\lambda}\right)\tan\alpha\right]. \tag{5}$$

[9] The internal and basal Hubbert-Rubbey fluid pressure ratios λ and λ_b are defined in *Davis et al.* [1983] as

$$\lambda = \frac{P - \rho_w g D}{|\sigma_z| - \rho_w g D}, \quad \lambda_b = \frac{P_b - \rho_w g D}{|\sigma_z| - \rho_w g D}, \tag{6}$$

where ρ and ρ_w are the wedge material and water densities and D is the water depth. The equations describing the whole envelope are provided by *Lehner* [1986]. The critical taper theory is assumed to be applicable to curved megathrust provided the wedge thickness is small compared to the radius of curvature as is the case here [*Cubas et al.*, submitted].

[10] The taper geometry and associated uncertainties were determined using the slab 1.0 model of *Hayes et al.* [2012] and the ETOPO1 topography [*Amante and Eakins*, 2009] (resolution 1′). The frontal part of the taper follows a critical envelope (Figure 2a) consistent with the evidence for internal deformation of the wedge reflected in the seismic profile (Figure 1e) and the seismicity before Tohoku-Oki (Figure 1b). We select this portion of the profile and determine the model parameters that predict a theoretical envelope that best reproduces the observed covariation of α and β. Probability densities of the three independent model parameters, the internal friction, the internal pore pressure ratio, and the effective basal friction defined as $\mu_b^{\text{eff}} = \tan\phi_b^{\text{eff}} = (1-\lambda_b)\tan\phi_b$ are plotted in Figure 2c and a table with the best fitting values is given in the supporting information. The best fitting model shows a high pore pressure ratio in the wedge ($\lambda = 0.8$), a standard internal friction ($\phi_{\text{int}} = 38.75°$, $\mu_{\text{int}} = 0.8$) and a low effective basal friction ($\phi_b^{\text{eff}} = 7.5°$, $\mu_b^{\text{eff}} = 0.13$). However, because of the trade off between ϕ_{int} and λ, these two parameters are poorly constrained. If we impose ϕ_{int} to be in the standard range of internal friction angles measured in the lab ($30° < \phi_{\text{int}} < 40°$, $0.57 < \mu_{\text{int}} < 0.84$, *Byerlee* [1978]), we get $0.22 < \lambda < 0.84$ at the 68% confidence level with the probability distribution peaking at $\lambda = 0.7$. For a rock density of 2800 kg/m^3, λ cannot be smaller than 0.35; lower values were considered here for the inversion purpose. The effective basal friction is constrained to be very low $5.7° < \phi_b^{\text{eff}} < 17.7°$ ($0.1 < \mu_b^{\text{eff}} < 0.32$) at the 68% confidence level with the probability distribution peaking at 8.25° ($\mu_b^{\text{eff}} = 0.14$). Its probability distribution does not vary much if ϕ_{int} is kept constant. Since the internal friction and pore pressure are now constrained, we evaluate the effective basal friction so that the extensional

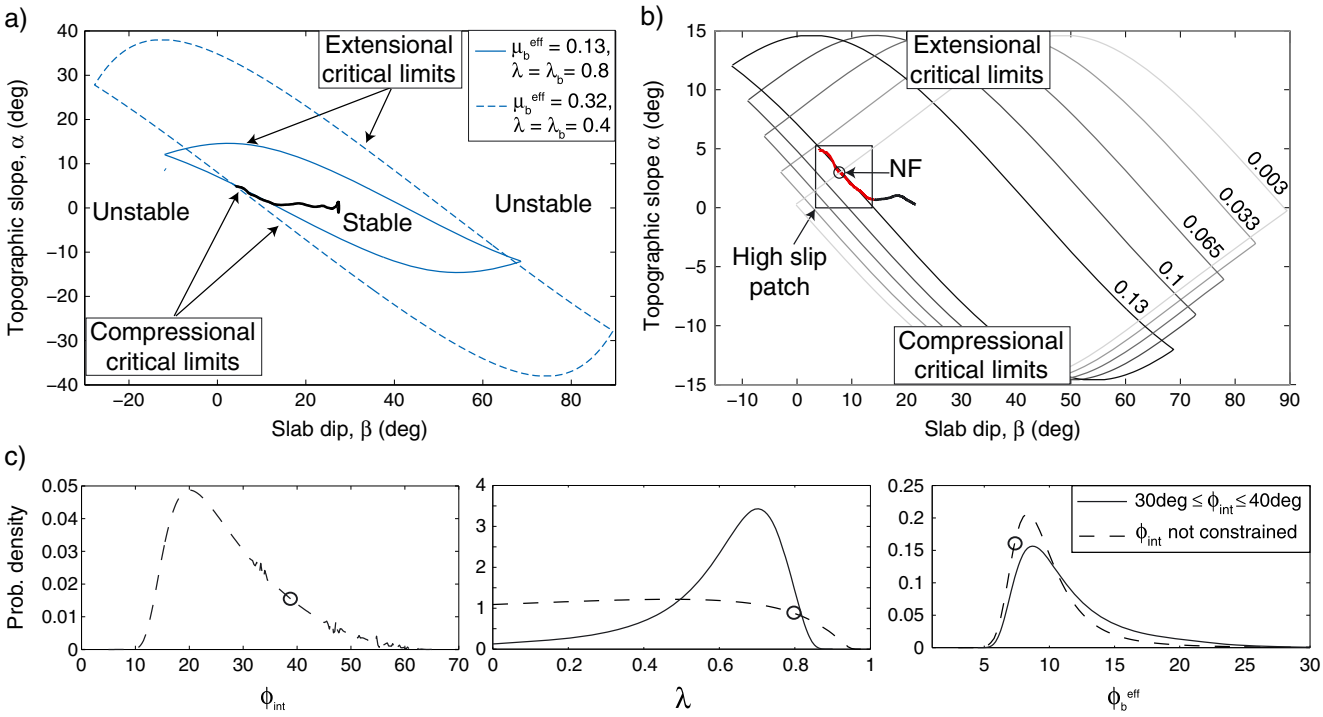

Figure 2. (a) Theoretical critical envelopes for two different sets of frictional properties compared to the taper of the swath profile of the studied area (ϕ_{int}=38.75°). (b) The portion of the taper considered at critical state is overlined in red and corresponds to the high slip patch of the Tohoku-Oki earthquake. The effective basal friction is decreased in order to reach the extensional limit for the taper measured at the location of the landward normal fault (NF) marked by a black circle (ϕ_{int}=38.75°, λ=0.8). (c) Probability densities for the three independent parameters ϕ_{int}, ϕ_b^{eff} and λ_{int} without constraints on ϕ_{int} (dashed line), for ϕ_{int} in the 30°–40° range (plain line). The densities are determined from fitting the portion of the wedge presumed to be at critical state with the theoretical envelope. Best fit values of the three parameters inversion are marked by a black circle.

critical state is reached for the taper angle measured at the location of the landward normal fault. A decreased effective basal friction μ_b^{eff} = 0.003 is required (Figure 2b). If the intrinsic friction is maintained, then the pore pressure would need to have increased from λ = 0.8 to 0.995. If the pore pressure is maintained, then the friction angle would need to have dropped from ϕ_b = 33.3° to 2.3° (μ_b = 0.66 to 0.04). Such a low friction could have resulted from very efficient dynamic weakening, as suggested by some aspects of the rupture [*Ide et al.*, 2011], possibly the results of thermal pressurization [*Noda and Lapusta*, 2013]. The extensional state would then be the result of a static coseismic stress change [*Kimura et al.*, 2012; *Conin et al.*, 2012; *Wang et al.*, 2010]. Dynamic branching could also be invoked but the aftershocks with normal faulting mechanisms suggest that horizontal extension must have resulted from the static stress change, justifying a static stress equilibrium analysis. However, since the taper trajectory is not parallel

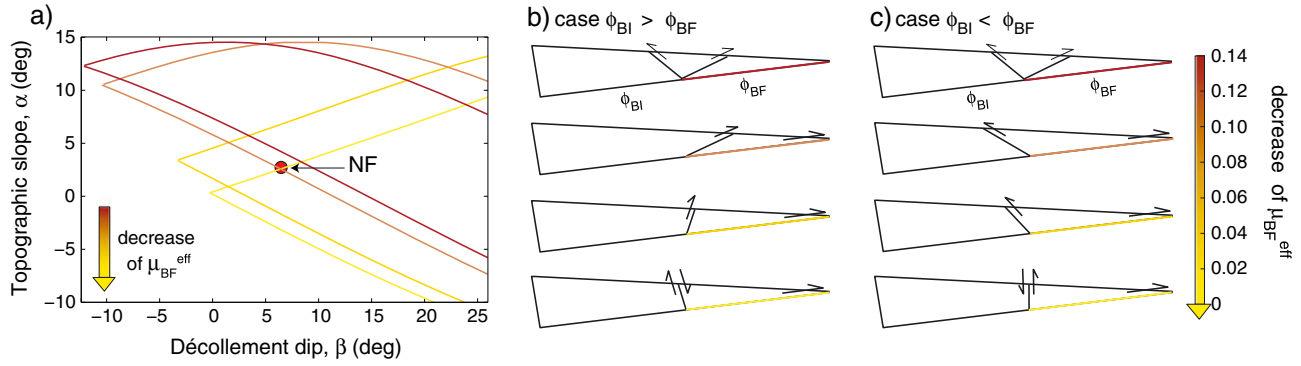

Figure 3. (a) Critical envelopes representative of the frontal part of the wedge of Figures 3b and 3c (for ϕ_{int}=38.75°, λ_{int}=0.8, and decreasing μ_{BF}^{eff} from 0.135, to 0.13, 0.037, and 0.003). The taper at the location of the normal fault (NF) is indicated by the red circle. Expected associated splay faults in the case of a spatial (b) decrease or (c) increase of the basal friction, for the different effective frontal basal frictions μ_{BF}^{eff} of Figure 3a.

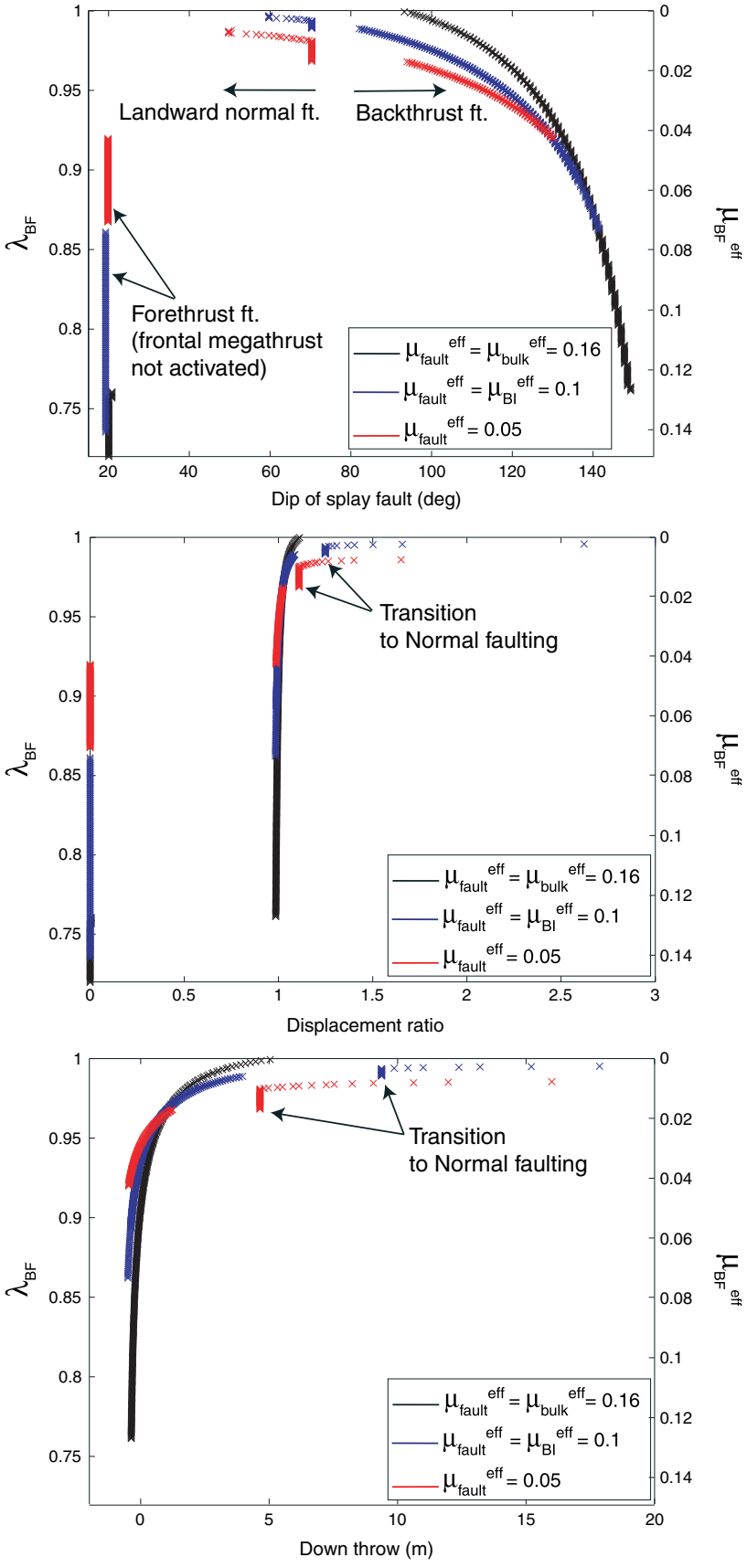

Figure 4. (a) Dip angle of splay fault formed due to a difference in effective basal friction beneath the inner and outer wedge, (b) Ratio between the slip beneath the outer wedge and the slip beneath the inner wedge, and (c) down throw along the splay fault for 50 m of slip along the outer wedge, as functions of the frontal pore pressure λ_{BF} or the effective frontal basal friction coefficient μ_{BF}^{eff}.

to the extensional branch of the envelope, it is not clear that the critical Coulomb wedge model is applicable to this analysis. Also, if the same properties apply to the whole outer wedge, the frontal part of the wedge should then collapse due to internal normal faulting, and slip should gradually increase toward the trench which is not observed. Actually, it is probably incorrect to assume that the whole wedge has been brought to the verge of failure in extension. We therefore explore that alternative explanation that the normal fault would rather be interpreted as a splay fault formed related to changes in frictional properties along the Megathrust [*Pons and Leroy* 2012; *Cubas et al.,* submitted].

3. Splay Faults as Markers for Transition of Frictional Properties

[11] We use here the limit analysis which is based on the principle of virtual powers and the theorem of maximum rock strength [*Chandrasekharaiah and Debnath*, 1994; *Salençon*, 2002; *Maillot and Leroy*, 2006]. The method investigates all possible collapse scenarios and selects the optimal one leading to the least upper bound to the tectonic force. The wedge strength is assumed to be determined by the Coulomb criterion. Compared with the critical taper theory, there is no need to assume homogeneous mechanical properties or a wedge uniformly at critical state. We used the formulation for saturated porous media from *Pons and Leroy* [2012] (supporting information). We assume that the basal pore pressure and basal friction vary abruptly at the transition from the inner to the outer wedge. We then determine the faulting pattern that develops at this transition. The resultant splay fault can be a forethrust, a backthrust, a seaward normal fault or a landward normal fault. Each of them could be associated with a conjugate fault. Conditions for each mechanism are summarized in Figure 3 where ϕ_{BI} and ϕ_{BF} are the basal friction angles, and λ_{BI} and λ_{BF} the pore pressure ratios of the internal and frontal part of the Megathrust, respectively. We use the properties found based on the critical taper theory for the bulk and the inner wedge Megathrust ($\mu_{int} = 0.8$, $\mu_{BI}^{eff} = 0.13$). The inner Megathrust pressure ratio is set equal to the internal pressure ratio ($\lambda_{BI} = \lambda_{int} = 0.8$). To account for dynamic weakening during seismic sliding, we decrease the effective basal friction μ_{BI}^{eff} from 0.13 to 0.1. The down-dip part of the wedge is thus in a stable state. Two possibilities are studied: in the first case, the basal friction coefficient angle decreases toward the trench $\phi_{BI} > \phi_{BF}$ (Figure 3b), in the second case, it increases $\phi_{BI} < \phi_{BF}$ (Figure 3c). We also vary the pore pressure along the frontal part of the Megathrust, hence, the effective basal frontal friction μ_{BF}^{eff}. If the effective frontal basal friction is too large ($\mu_{BF}^{eff} > 0.13$), the taper is then in the unstable field (Figure 3a), no sliding is allowed along the updip part of the wedge and conjugate thrust faults are formed at the transition in order to increase the taper (Figure 3b and 3c). If the effective frontal basal friction decreases and the wedge reaches the compressional limit ($\mu_{BF}^{eff} = 0.13$), the décollement is then fully activated, and a thrust fault appears at the transition to accommodate the difference of slip along the upper and lower part of the Megathrust generated by the difference in basal friction. For $\phi_{BI} > \phi_{BF}$, a shallow dipping forethrust is formed (25°), while $\phi_{BI} < \phi_{BF}$ leads to a backthrust (149.5°). If the effective frontal basal friction is decreased, the frontal wedge enters the stable domain, and forethrust and backthrust get steeper (for $\mu_{BF}^{eff} = 0.037$, dips are of 72° and 132°, respectively). By decreasing more the effective friction, we reach the extensional critical limit ($\mu_{BF}^{eff} = 0.003$) and dips increase again resulting in a seaward normal fault for $\phi_{BI} > \phi_{BF}$, and a quasi-vertical normal fault for $\phi_{BI} < \phi_{BF}$.

[12] Since a larger basal friction angle and basal pore pressure are required along the updip portion to activate a landward normal fault, we investigate more systematically cases with $\phi_{BI} < \phi_{BF} < \phi_{int}$, and $\lambda_{BI} < \lambda_{BF} < 1$. In Figure 4a, different effective frictions along the splay fault are tested. If we assign to the splay fault the properties of the bulk, a quasi-vertical normal fault can be obtained for $0.0006 < \mu_{BF}^{eff} < 0.003$ ($0.995 < \lambda_{BF} < 0.999$ if $\phi_{BF} = 28°$). For the same friction and pore pressure ratio than the down-dip Megathrust, a 70° to 60° landward normal fault can be obtained for $0.002 < \mu_{BF}^{eff} < 0.005$ ($0.994 < \lambda_{BF} < 0.996$ if $\phi_{BF} = 28°$). If the splay fault is weaker ($\mu_{Fault}^{eff} = 0.05$), landward normal faults with dips ranging from 70° to 50° are obtained for $0.0065 < \mu_{BF}^{eff} < 0.015$ ($0.968 < \lambda_{BF} < 0.987$ if $\phi_{BF} = 28°$), conditions for which the outer wedge would be far from the extensional state.

[13] Assuming that the ratio between the internal and frontal virtual velocities derived from the limit analysis is equal to the ratio of actual displacement between the internal and frontal parts of the wedge, we can estimate the down throw along the splay fault as a function of the frictional properties. The ratio can reach up to 2.5 for a weak splay fault and conditions near extensional collapse (Figure 4b). For a 70° dipping fault, the ratio ranges between 1.2 and 1.4. In the case of a 50 m displacement of the outer wedge, the inner wedge displacement would then range between 33 to 42 m and the down throw generated by the normal fault between 5 to 10 m (Figure 4c), consistent with observations from *Tsuji et al.* [2011, 2013]. These numbers need to be considered with caution as they are derived from a quasi-static force balance.

4. Discussion and Conclusion

[14] The critical taper theory [*Davis et al.*, 1983; *Dahlen*, 1984] requires a relatively high internal pore pressure ratio in the epicentral area of the Tohoku-Oki earthquake ($\lambda = 0.7 + 0.14/ - 0.48$ give 68% range, for ϕ_{int} in the 30°–40° range) with a preferred value of $\lambda = 0.8$ as well as a low effective basal friction ($0.1 < \mu_b^{eff} < 0.32$ at the 68% confidence level) with a preferred value of $\mu_b^{eff} = 0.13$. A coseismic decreased effective friction $\mu_b^{eff} < 0.003$ induced by frictional weakening would allow the wedge to reach the extensional state at the normal fault location. The state of stress within the outer wedge would then vary from a compressional state in the interseismic period to extensional following the coseismic displacement. However, we note that the taper trajectory is not parallel to the extensional branch of the critical envelope. If basal friction is uniformly reduced enough so that the critical branch in extension intersect the taper trajectory, the whole portion of the wedge updip on this intersection would collapse so as to follow the extensional critical branch. As would happen in the case of a uniform critical taper, distributed horizontal extension throughout the wedge would be expected. One way to reconcile the observations and our interpretations is to assume

a change of basal frictional properties from the inner to the outer wedge. Our analysis shows that a slight increase of the friction coefficient associated to a strong increase of the basal pore pressure would allow for the activation of a 50° to 70° dipping landward normal fault at the transition. The lower updip effective basal friction ($0.002 < \mu_b^{\text{eff}} < 0.015$) would enable a larger displacement along the outer wedge (1.2 to 1.5 the inner wedge displacement) and permit 5 to 10 m of vertical displacement along the normal fault in good agreement with bathymetric observations [*Tsuji et al.*, 2011, 2013]. This down throw implies a relatively small volume of displaced water compared to 50 m of displacement along a 60 to 70 km length of the Megathrust. Most probably, the normal fault did not contribute much to the tsunami. The low effective basal friction inferred in this study is also consistent with the dynamic overshoot proposed by *Ide et al.* [2011] and could have resulted from thermal pressurization of the updip part of the megathrust as suggested by *Noda and Lapusta* [2013]. By contrast, the long term high pore pressure along the Megathrust could be a permanent feature maintained by continuous dehydration of siliceous sediments and clays dragged along the Megathrust [*Kimura et al.*, 2012] and by a low permeability. The different effective friction coefficient beneath the inner and outer wedge could reveal a different mineralogy resulting in a more efficient updip dynamic thermal pressurization and thus a dynamic increase of the pore pressure beneath the outer wedge.

[15] After activation of slip along the Megathrust, the compressional stress must build up again to bring the outer wedge back to a critical state. The stress build up can result from interseismic strain or, more probably, from the stress transfer due to ruptures along the deeper portion of the Megathrust, similar to the numerous Mw < 7.5 earthquakes reported historically [*Hashimoto et al.*, 2009], and afterslip [*Hu and Wang*, 2008].

[16] These normal faults have often been interpreted as a consequence of basal erosion [e.g., *Von Huene et al.*, 2004]. Our interpretation might provide an alternative general explanation for the normal faulting aftershocks sometimes observed after such earthquakes [e.g., *McKenzie and Jackson*, 2012] and for the presence of normal faults at the transition between outer and inner wedges [*Krabbenhöft et al.*, 2004; *Klaeschen et al.*, 1994]. Normal faulting would then be an indicator of updip propagation of earthquakes.

[17] **Acknowledgments.** This project was supported by the National Science Foundation through grant EAR-1118239 and by the Gordon and Betty Moore Foundation through grant GBMF 423.01 to the Caltech Tectonics Observatory. This is Tectonics Observatory contribution # 235.

[18] The Editor thanks two anonymous reviewers for their assistance in evaluating this paper.

References

Amante, C., and B. W. Eakins (2009), ETOPO1 1 Arc-minute global relief model: Procedures, data sources and analysis. NOAA Technical Memorandum NESDIS NGDC-24, 19 p.

Asano, Y., T. Saito, Y. Ito, K. Shiomi, H. Hirose, T. Matsumoto, S. Aoi, S. Hori, and S. Sekiguchi (2011), Spatial distribution and focal mechanisms of aftershocks of the 2011 off the Pacific coast of Tohoku Earthquake, *Earth Planets Space*, *63*(7), 669–673, doi:10.5047/eps.2011.06.016.

Byerlee, J. D. (1978), Friction of rocks, *Pure Appl. Geophys.*, *116*, 615–626.

Chandrasekharaiah, D. S., and L. Debnath (1994), *Continuum Mechanics*, Academic Press, Inc., San Diego, Calif.

Conin, M., P. Henry, V. Godard, and S. Bourlange (2012), Splay fault slip in a subduction margin, a new model of evolution, *Earth Planet. Sci. Lett.*, *341-344*, 170–175, doi:10.1016/j.epsl.2012.06.003.

Dahlen, F. A. (1984), Noncohesive critical Coulomb wedges: An exact solution, *J. Geophys. Res.*, *89*, 10,125–10,133.

Davis, D. M., J. Suppe, and F. A. Dahlen (1983), Mechanics of fold-and-thrust belts and accretionary wedges, *J. Geophys. Res.*, *88*, 1153–1172.

Fujiwara, T., S. Kodaira, T. No, Y. Kaiho, N. Takahashi, and Y. Kaneda (2011), The 2011 Tohoku-Oki earthquake: Displacement reaching the trench axis, *Science*, *334*, 1240, doi:10.1126/science.1211554.

Hashimoto, C., A. Noda, T. Sagiya, and M. Matsuura (2009), Interplate seismogenic zones along the Kuril-Japan trench inferred from GPS data inversion, *Nature Geosci.*, *2*, 141–44.

Hayes, G. P., D. J. Wald, and R. L. Johnson (2012), Slab1.0: A three-dimensional model of global subduction zone geometries, *J. Geophys. Res.*, *117*, B01302, doi:10.1029/2011JB008524.

Hu, Y., and K. Wang (2008), Coseismic strengthening of the shallow portion of the subduction fault and its effects on wedge taper, *J. Geophys. Res.*, *113*, B12411, doi:10.1029/2008JB005724.

Ide, S., A. Baltay, and G. C. Beroza (2011), Shallow dynamic overshoot and energetic deep rupture in the 2011 Mw 9.0 Tohoku-oki earthquake, *Science*, *332*, 1426–1429, doi:10.1126/science.1207020.

Ito, Y., T. Tsuji, Y. Osada, M. Kido, D. Inazu, Y. Hayashi, H. Tsushima, R. Hino, and H. Fujimoto (2011), Frontal wedge deformation near the source region of the 2011 Tohoku-oki earthquake, *Geophys. Res. Lett.*, *38*, L00G05, doi:10.1029/2011GL048355.

Kimura, G., S. Hina, Y. Hamada, J. Kameda, T. Tsuji, M. Kinoshita, and A. Yamaguchi (2012), Runaway slip to the trench due to rupture of highly pressurized megathrust beneath the middle trench slope: The tsunamigenesis of the 2011 Tohoku earthquake off the east coast of northern Japan, *Earth Planet. Sci. Lett.*, *339-340*, 32–45, doi:10.1016/j.epsl.2012.04.002.

Klaeschen, D., I. Belykh, H. Gnibidenko, S. Patrikeyev, and R. von Huene (1994), Structure of the Kuril Trench from seismic reflection records, *J. Geophys. Res.*, *88*, 24,173–24,188, doi:10.1029/94JB01186.

Krabbenhöft, A., J. Bialas, H. Kopp, N. Kukowski, and C. Hubscher (2004), Crustal structure of the Peruvian continental margin from wide-angle seismic studies, *Geophys. J. Int.*, *159*, 749–764, doi:10.1111/j.1365-246X.2004.02425.x.

Lehner, F. K. (1986), Comments on noncohesive critical Coulomb wedges: An exact solution, *J. Geophys. Res.*, *9*, 793–796.

Loveless, J. P., and B. J. Meade (2011), Spatial correlation of interseismic coupling and coseismic rupture extent of the 2011 Mw 9.0 Tohoku-oki earthquake, *Geophys. Res. Lett.*, *38*, L17306, doi:10.1029/2011GL048561.

Maillot, B., and Y. M. Leroy (2006), Kink-fold onset and development based on the maximum strength theorem, *J. Mech. Phys. Solids*, *54*, 2030–2059.

McKenzie, D., and J. Jackson (2012), Tsunami earthquake generation by their lease of gravitational potential energy, *Earth Planet. Sci. Lett.*, *345–348*, 1–8, doi:10.1016/j.epsl.2012.06.036.

Noda, H., and N. Lapusta (2013), Stable creeping fault segments can become destructive as a result of dynamic weakening, *Nature*, *493*, 518–521, doi:10.1038/nature11703.

Oleskevich, D. A., R. D. Hyndman, and K. Wang (1999), The updip and downdip limits to great subduction earthquakes: Thermal and structural models of Cascadia, south Alaska, SW Japan, and Chile, *J. Geophys. Res.*, *104*, 14,965–14,991, doi:10.1029/1999JB900060.

Ozawa, S., T. Nishimura, H. Suito, T. Kobayashi, M. Tobita, and T. Imakiire (2011), Coseismic and postseismic slip of the 2011 magnitude 9 Tohoku-Oki earthquake, *Nature*, *117*, 373–376, doi:10.1038/nature10227.

Pons, A., and Y. M. Leroy (2012), Stability of accretionary wedges based on the maximum strength theorem for fluid-saturated porous media, *J. Mech. Phys. Solids*, *60*, 643–664, doi:10.1016/j.jmps.2011.12.011.

Salençon, J. (2002), Del Elasto-Plasticité au Calcul à la Rupture, Ellipses, Paris, 264 p.

Simons, M., et al. (2011), The 2011 magnitude 9.0 Tohoku-Oki earthquake: Mosaicking the megathrust from seconds to centuries, *Science*, *332*, 1421–1425.

Suppe, J. (2007), Absolute fault and crustal strength from wedge tapers, *Geology*, *35*, 1127–1130, doi:10.1130/G24053A.1.

Tsuji, T., Y. Ito, M. Kido, Y. Osada, H. Fujimoto, J. Ashi, M. Kinoshita, and T. Matsuoka (2011), Potential tsunamigenic faults of the 2011 Tohoku earthquake, *Earth Planet Space*, *63*, 831–834, doi:10.5047/eps.2011.05.028.

Tsuji, T., K. Kawamura, T. Kanamatsu, T. Kasaya, K. Fujikura, Y. Ito, T. Tsuru, and M. Kinoshita (2013), Tohoku-oki earthquake: The role of extensional faulting in the generation of a great tsunami, *Earth Planet. Sci. Lett.*, *364*, 44–58, doi:10.1016/j.epsl.2012.12.038.

Von Huene, R., C. R. Ranero, and P. Vannucchi (2004), Generic model of subduction erosion, *Geology*, *32*, 913–916, doi:10.1130/G20563.1.

Wang, K., Y. Hu, R. von Huene, and N. Kukowski (2010), Interplate earthquakes as a driver of shallow subduction erosion, *Geology*, *38*, 431–434, doi:10.1130/G30597.1.

Wei, S., R. Graves, D. Helmberger, J. P. Avouac, and J. Jiang (2012), Sources of shaking and flooding during the Tohoku-Oki earthquake: A mixture of rupture styles, *Earth Planet. Sci. Lett.*, *333-334*, 91–100, doi:10.1016/j.epsl.2012.04.006.